# Guided Wave Optics Laboratory

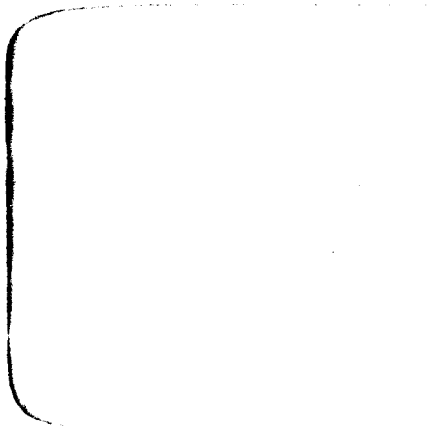

## Department of Electrical and Computer Engineering

**University of Colorado at Boulder**
**Boulder, Colorado**



**Report No. 63**

# Study of UV Bleached Channel Waveguide Performance in NLO Polymer Films

Wei Feng, Sihan Lin, R. Brian Hooker,
and Alan R. Mickelson

**October 1994**

**Guided Wave Optics Laboratory**
**Department of Electrical and Computer Engineering**
**University of Colorado at Boulder**
**Boulder, Colorado 80309-0425**

This work was supported by the National Science Foundation under Contract #ECS-9015752, the Office of Naval Research under Contract #N00014-92-J-1190, and the Army Research Office under Contract #DAAL-03-92-G-0289.

unclassified
SECURITY CLASSIFICATION OF THIS PAGE



# REPORT DOCUMENTATION PAGE

Form Approved OMB No. 0704-0188

| | |
|---|---|
| 1a. REPORT SECURITY CLASSIFICATION: unclassified | 1b. RESTRICTIVE MARKINGS: none |
| 2a. SECURITY CLASSIFICATION AUTHORITY: DISCASS | 3. DISTRIBUTION/AVAILABILITY OF REPORT: unrestricted |
| 2b. DECLASSIFICATION/DOWNGRADING SCHEDULE: N/A | |
| 4. PERFORMING ORGANIZATION REPORT NUMBER(S): ECE/CWOL/63 | 5. MONITORING ORGANIZATION REPORT NUMBER(S): DOD-ONRN00014-92-J-1190 |
| 6a. NAME OF PERFORMING ORGANIZATION: University of Colorado; 6b. OFFICE SYMBOL (If applicable): | 7a. NAME OF MONITORING ORGANIZATION: Office of Naval Research, Attn: Dr. Arthur Jordan, Code 1114 SE |
| 6c. ADDRESS (City, State, and ZIP Code): Electrical & Computer Engineering Dept., Boulder, CO 80309-0425 | 7b. ADDRESS (City, State, and ZIP Code): 800 N. Quincy Avenue, Arlington, VA 22217-5000 |
| 8a. NAME OF FUNDING/SPONSORING ORGANIZATION: Office of Naval Research; 8b. OFFICE SYMBOL (If applicable): | 9. PROCUREMENT INSTRUMENT IDENTIFICATION NUMBER |
| 8c. ADDRESS (City, State, and ZIP Code): 800 N. Quincy Avenue, Arlington, VA 22217-5000 | 10. SOURCE OF FUNDING NUMBERS: PROGRAM ELEMENT NO. / PROJECT NO. / TASK NO / WORK UNIT ACCESSION NO. |

11. TITLE (Include Security Classification)

(u) Study of UV Bleached Channel Waveguide Performance in NLO Polymer Films

12. PERSONAL AUTHOR(S)

Wei Feng, Sihan Lin, R. Brian Hooker, and Alan R. Mickelson

| 13a. TYPE OF REPORT | 13b. TIME COVERED | 14. DATE OF REPORT (Year, Month, Day) | 15. PAGE COUNT |
|---|---|---|---|
| manuscript | FROM _____ TO _____ | 10/1994 | 30 |

16. SUPPLEMENTARY NOTATION

| 17. COSATI CODES | | |
|---|---|---|
| FIELD | GROUP | SUB-GROUP |
| | | |
| | | |

18. SUBJECT TERMS (Continue on reverse if necessary and identify by block number)

DISTRIBUTION STATEMENT A
Approved for public release;
Distribution Unlimited

19. ABSTRACT (Continue on reverse if necessary and identify by block number)

We report the studies on UV photo bleached uptical channel waveguides in nonlinear optical polymer films. The nonlinear optical polymer used is PMMA/DR1 side chain polymer. Effective indices of the channel waveguides are measured with prism coupling technique along with the effective indices of the bleached and unbleached polymer films. The effective index method was used to predict the effective indices of the channel waveguides from measurements of the slab waveguides without detailed knowledge of the index distributions in the polymer films. Some local effects on the boundaries of the channel waveguides caused by the UV bleaching process are identified with the comparison between direct channel measurement and prediction. It is found that the technique used in this paper can be employed to predict the performance of the channel waveguides processed with proper bleaching process.

| 20. DISTRIBUTION/AVAILABILITY OF ABSTRACT | 21. ABSTRACT SECURITY CLASSIFICATION |
|---|---|
| ■ UNCLASSIFIED/UNLIMITED ☐ SAME AS RPT. ☐ DTIC USERS | unclassified |
| 22a. NAME OF RESPONSIBLE INDIVIDUAL: Alan R. Mickelson | 22b. TELEPHONE (Include Area Code): 303/492-7539; 22c. OFFICE SYMBOL: |

DD Form 1473, JUN 86 — Previous editions are obsolete. — SECURITY CLASSIFICATION OF THIS PAGE

# Study of UV Bleached Channel Waveguide Performance in NLO Polymer Films

Wei Feng, Sihan Lin, R. Brian Hooker and Alan R. Mickelson

## Abstract

We report the studies on UV photo bleached optical channel waveguides in nonlinear optical polymer films. The nonlinear optical polymer used is PMMA/DR1 side chain polymer. Effective indices of the channel waveguides are measured with prism coupling technique along with the effective indices of the bleached and unbleached polymer films. The effective index method was used to predict the effective indices of the channel waveguides from measurements of the slab waveguides without detailed knowledge of the index distributions in the polymer films. Some local effects on the boundaries of the channel waveguides caused by the UV bleaching process are identified with the comparison between direct channel measurement and prediction. It is found that the technique used in this paper can be employed to predict the performance of the channel waveguides processed with proper bleaching process.

The authors are with the Department of Electrical and Computer Engineering, University of Colorado at Boulder, Boulder, CO 80309

# I. INTRODUCTION

There are many ways of fabricating optical channel waveguides in nonlinear optical polymer films, such as ultraviolet (UV) photo bleaching[1,2], reactive ion etching[3,4], and laser ablation[5]. UV illumination lowers the index of refraction of the exposed NLO polymer. Light is confined in the channel because of the higher index of refraction of polymer in the channel. There are advantages of using UV photo bleaching. The index changes of the bleached polymer can be controlled by the exposure, so the index contrast between the core and the cladding of a channel waveguide can be adjusted to the desired values. In addition, UV bleaching forms channel waveguides inside the polymer film, by a purely planar technology allowing for the possibility of multilayer structures to be fabricated one layer at a time.

Characterizing optical waveguides is important for the design and fabrication of integrated optical devices such as directional couplers. The propagation constant or the effective index of the optical waveguide is an important parameter to know. To find the effective index of the optical waveguide, one can use methods for solving the wave equations which require the knowledge of the index distribution of the waveguide. The effective index method[6,7], or other numerical methods such as beam propagation method[8], finite difference method, and finite element method[9,10] are frequently used.

The index distribution of the unbleached polymer film can, in general, be assumed to be uniform across the film. However, the index distribution of the bleached film apparently is not uniform because the film is highly absorptive at the bleaching wavelengths, making the intensity of the UV light not uniform in depth through the film[2,11]. Because of these complex effects of the UV bleaching process on the NLO polymer, it is difficult to characterize the index distribution of a UV bleached polymer film accurately. There are some methods which can be used to find the index distributions such

as inverse WKB method using many measured effective indices[12], and the near-field measurement method[13]. These techniques, however, are limited in accuracy and generality.

With the help of the prism coupling technique to directly measure the effective indices of slab and channel waveguides, the effective index method can be effective (as long as the waveguide is far from cutoff) for analysis of UV bleached channel waveguides in polymer films, because characterizing the index distribution of the bleached polymer film becomes unnecessary. According to the effective index method, as will be shown later, only the effective indices of the bleached and unbleached films are required to calculate the effective index of the channel waveguide.

## II. METHODS OF PREDICTION AND MEASUREMENT

In a UV photo bleached polymer waveguide, the way of describing the index distribution can be simplified by assuming the UV bleached channel geometry is rectangular, as shown in Figure 1. There is in general a film thickness difference between the unbleached and bleached regions due to the film thickness shrinkage in the bleached regions. Figure 2 shows the change of effective index of the bleached film with various bleaching times. Further, the effective index method can be applied to this channel geometry easily to predict the effective index of the channel waveguide from the knowledge of the effective indices in the different polymer regions. According to the effective index method, the UV bleached channel waveguide (Figure 3a) can be divided into three regions I,II,III. This splits the two dimensional (2-D) channel waveguide problem into three 1-D problems (in regions I,II,III, respectively). We can solve these 1-D slab problems easily to give the effective indices $n_{e1}$, $n_{e2}$, $n_{e1}$ from the known index distributions(Figure 3b)[14]. Finally, the problem becomes a final 1-D slab waveguide problem with the index

distribution shown in Figure 3c, and can be solved to give the final effective index of the channel waveguide.

For unbleached films, index distributions can be assumed uniform across the film. The actual index of the polymer film can be calculated from the measured effective indices when there are more than one mode, or the actual index can be calculated with the measured effective index and known thickness, when there is only one mode[14]. However, for bleached films, the index distribution is not uniform in depth[2,11]. It is hard to characterize the index distribution accurately from measured effective indices. The effective index method is very powerful in this case because there is no need to know the index distribution in depth in the polymer film. As shown in Figure 3, if the effective indices of regions I, II, III are measured directly from M-line measurements, steps a) and b) in Figure 3 can be skipped and the effective index of the channel waveguide can be calculated starting from step c). Therefore it is not necessary to characterize the index distribution in the bleached regions.

In order to make consistent measurement and predictions, a mask is made that contains straight channel waveguides of various widths as well as large regions of bleached and unbleached slab waveguides. Hence a single sample contains all the key structures we wish to measure. Figure 4 shows the structure on a sample after processing. Next to the bleached optical channel waveguides, there are large bleached and unbleached regions over which the effective indices of the slab waveguides are measured. Since the indices of the mask-covered polymer regions remain unchanged, the effective index in the channel region (region II in Figure 3b) is assumed to be that of the unbleached region . Therefore, the effective index of the channel can be calculated by the effective index method using the effective indices measured in the bleached and unbleached regions.

The effective indices of slab or channel waveguides can be measured with the prism coupling technique (M-line measurement)[15,16]. Figure 5 shows two kinds of M-line setups. The setup shown in Figure 5a is used mostly in effective index measurement of

slab waveguides. The setups shown in Figure 5b,c are used for either slab or channel effective index measurement.

The first is used by launching light from one side of the prism and monitoring the power of the reflected beam from the other. By changing the incident angle $\phi$ with respect to the normal of the incident surface of the prism, one can find a power minimum which occurs when the light hits the surface at an angle which excites one specific mode. Using this angle, the corresponding effective index can be calculated with Equation (1)

$$n_{eff} = n_{prism} \sin\left[\alpha + \sin^{-1}\left(\frac{\sin\varphi}{n_{prism}}\right)\right] \qquad (1)$$

where $n_{prism}$ is the index of refraction of the prism, $\alpha$ is the corner angle of the prism, and $n_{eff}$ is the effective index of the mode in the waveguide.

In the setup shown in Figure 5b,c, the light is launched into either the channel or the slab waveguide by fiber-butt coupling. From the output side of the prism, the mode spectrum of the launched modes is displayed on the screen or a CCD camera. By measuring the angles of the output beams with respect to the normal of the prism surface, effective indices of the corresponding modes can also be calculated using Equation (1). Either channel or slab modes can be excited and measured by changing the input fiber position.

There are some other advantages of using setups in Figure 5b,c over the setup in Figure 5a. With setups in Figure 5b,c, the M-lines are shown on the screen. By adjusting the pressure of the piston on the sample while observing the M-lines, the shift and broadening effects of the M-lines[17] can be minimized, resulting in more accurate measurements. These effects are more pronounced for polymer films. Even though the setup in Figure 5b is popular in the measurement of waveguides in glass or $LiNbO_3$[16], we find that due to the softness of the polymer film, the pressure of the piston distorts the

sample against the corner of the prism where the coupling happens. This deformation of the film and channel waveguides results in a significant shift and broadening of M-lines. Adoption of the setup in Figure 5c minimizes these problems.

## III. MEASUREMENT AND RESULTS

The detailed setup is shown in Figure 6. Light from 0.824 μm laser is launched into the sample through the fiber. A polarization controller is used to control the polarization of the input light. The fiber output end is mounted on the rotary stage with the prism through an x-y-z stage, and can be moved with respect to the sample by adjusting this x-y-z stage. The sample is pressed against the prism by adjusting the piston. The prism coupler and the fiber holder are then mounted on a Klinger motorized rotary stage. The M-line from the prism is projected on the screen or a CCD camera about a meter away. In order to measure the angle of the M-line with respect to the normal of the surface of the prism, a He-Ne laser is used. As shown in Figure 6, the reflected He-Ne laser beam from the surface of the prism can be adjusted to coincide with the M-line by aligning the He-Ne laser and rotating the sample stage. We then record the reading of the angle on the rotary stage, and turn the stage until the reflected beam falls on the pin hole at the output of the He-Ne laser. The angle the stage turns is the angle of the M-line with respect to the surface of the prism. Directly imaging the M-lines onto the CCD camera gives in general better resolution in doing angle measurement. The prism used is a 45-45-90 prism made of LaSF9 Schott glass.

There are generally four sources of error in M-line measurement. From Equation (1), we see that any errors in these quantities $n_{prism}$, $\alpha$ and $\phi$ contribute to the uncertainty of the calculated effective index. Further the pressure of the prism against the sample causes a shift and broadening of the M-line, which in turn affects the measurement of $\phi$. The estimated absolute accuracy of our effective index measurement is about $\pm 1X10^{-3}$. In

this study, however, only the relative differences among the measurements are important. Errors from $n_{prism}$ and $\alpha$ can be ignored, and uncertainties of the results come only from measurement of $\phi$. One way to reduce the uncertainty of $\phi$ is to minimize the shift and broadening of the M-line. We can do this by reducing the pressure while monitoring the M-line on a TV screen. Our measurement uncertainty of the differences in effective indices is estimated about $\pm 2X10^{-4}$.

Samples are prepared with 20% by weight PMMA/DR1 side chain polymer, which has a glass transition temperature of about 125 °C. Polymer films are formed on the microscope glass slides by spin coating. The film is about 2.4 μm thick and baked at 90 °C for 3 hours and 110 °C for 12 hours. Seven optical channels are designed with the nominal widths from 2 μm to 8 μm with 1 μm increments(see Figure 4). The actual channel widths are measured with a microscope. The spacings between the channels are 200 μm, over which the polymer is bleached. Outside the channel regions, there are large areas where the polymer is not bleached. The UV source used is the large area UV illuminator from Oriel with broad band mid-UV light from a 350 W mercury lamp. The illumination intensity is 68 $mW/cm^2$.

After the films are prepared, samples are bleached through the contact mask to form channel waveguides under three different conditions: a) room temperature bleaching for 72 hours; b) high temperature bleaching at about 120°C for 50 hours; c) room temperature bleaching for 72 hours, and then further baking at 115°C for overnight. Since the bleaching rate is faster at high temperature, the sample for high temperature bleaching is kept under UV light for a shorter period of time to make the index changes close to the index changes made at room temperature.

Figures 7, 9 and 10 show the results of measurements and calculations on the samples processed under three different conditions: room temperature UV bleaching, high temperature bleaching close to the glass transition temperature, and room temperature bleaching and high temperature annealing (high temperature baking). Table 1 summaries

the agreements between the measured and calculated results on these waveguides. As will be explained later, room temperature bleaching produces reasonably good agreement for TE polarization. However, there is no agreement for TM polarization. High temperature bleaching always has poor agreement for both TE and TM polarizations. Process with room temperature bleaching and high temperature annealing results in the best agreement.

Figure 7 shows the measured effective indices of the channel waveguides and those of the slab regions of a sample bleached at room temperature. Each individual data point of the bleached film (slab waveguide) is measured at the area close to the corresponding channel waveguide. The solid curve is the prediction from measured effective indices in the bleached and unbleached regions based on the effective index method. It is noted that the bleached part of the film exhibits a very strong birefringence between TE and TM polarizations, and for TE-polarization (quasi-TE for channel waveguides), there is a significant index difference between the bleached and unbleached regions, which is crucial for forming the channel waveguide. The measurement of effective indices of the channel waveguides in TE polarization agrees reasonably well with the calculated values. However, for TM-polarization, the effective indices of the bleached slab regions do not decrease in comparison with that of unbleached regions (Figure 7b). In fact, there is a slight increase in the effective index in the bleached regions by about $1X10^{-3}$. According to the effective index method, it is not supposed to have any guided channel mode with this index distribution for TM polarization. However, the channel waveguides work well for both polarizations and the measured effective indices of the channels in TM polarization are much higher than both of those bleached and unbleached regions. Clearly calculations do not predict the waveguide performance.

The strong birefringence in this room temperature bleached film occurs because the UV bleaching is more effective on dye molecules aligned in the plane of the film and has smaller effect on molecules aligned perpendicular to the film. Since the UV bleaching is done at room temperature, there is little rotational mobility of the dye molecules. As a

result, the molecules aligned in the plane of the film are more likely to be bleached than those perpendicular to the film. Therefore the index in TM polarization does not decrease as much as that in TE polarization. The slight increase in effective index of TM polarization in the bleached film over the unbleached one can be explained by the fact that the film shrinkage is caused by the bleaching of the dye molecules aligned along the film, resulting in a density increase of the molecules aligned perpendicular to the film and an increase in its effective index (TM polarization). This process tends to bring some dye molecules from the in-plane orientation into the orientation perpendicular to the film, causing a increased effective index for TM polarization. The guided channel modes of TM polarization shown in Figure 7b can be explained by the occurrence of some strongly localized effects on the boundaries between bleached and unbleached regions, which are not detected in the slab M-line measurements. It is found that after UV bleaching, the polymer film in the bleached region shrinks in thickness by as much as 15%[18], while the polymer film in the unbleached region does not. At room temperature, the film is very elastic and barely viscous. The thickness difference on the boundaries causes stress perpendicular to the film over this area. This stress in turn causes stress induced index changes. Similar effects can be seen in some ion-exchange channel waveguides[19]. These effects happen only on the boundaries, and the slab measurements fail to detect them. Since the two boundaries of a channel waveguide are very close to each other, this stress induced index increase forms the channel waveguides shown in Figure 7b. In fact, even the boundaries between the bleached and unbleached slabs exhibits lateral light confinement (channel waveguide characteristics) through the curved M-lines in TM polarization, confirming that this stress on the boundaries are causing an increase in refractive index in TM polarization on that boundary.

Figure 8a is the surface profile made with an atomic force microscope(AFM) across a channel of a room temperature bleached sample. The strong ringing effect on the surface profile suggests that there is a stress built in due to shrinkage of the bleached film and the

elasticity of the film. Because of the complexity of the stress and the stress induced index changes on the boundaries, it is difficult to consider these effects in the simulation and to predict the channel waveguide performance of samples bleached at room temperature.

When the polymer film is heated close to its glass transition temperature, the dye molecules in the film tend to rotate randomly due to thermal excitations and the sample is more viscous and less elastic[20]. UV bleaching has similar effect on both TE and TM polarizations and the thickness shrinkage does not result in stress on the boundaries. Therefore the samples bleached under this condition are expected to exhibit smaller birefringence and a minimized stress-induced boundary effect. The residual birefringence between TE and TM polarizations is caused by the film constraints to the molecular alignment and the different TE and TM boundary conditions. Figure 9 shows the agreement between measurements and these expectations. However, it is found that the measured effective indices of the channel waveguides for both polarizations are always lower than those of predictions for all the channel widths. We believe that this is caused by the diffusion process during high temperature bleaching. Molecules in the sample with a temperature approaching its glass transition temperature have freedom to rotate and drift. Molecules drifting out of the channel region will be bleached, meanwhile the bleached molecules drift into channel region. The actual index in the channel region is lowered due to this effect during the long bleaching process. Therefore, the actual effective index in the channel region cannot be well represented by that in the large unbleached region. The resultant effective indices of these channel waveguides are lower than what are expected from slab measurement. Again these diffusion factors are difficult to quantify in predicting the channel performance.

Another way of fabricating the channel waveguides through UV bleaching is to bleach the sample at room temperature and then bake it at a high temperature close to its glass transition temperature. The second step can be considered as an "annealing" process. After the annealing, the dye molecules become randomly oriented and the bleached

molecules are more evenly distributed for TE and TM polarizations. Therefore the birefringence is minimized. At the same time, the stress in the original film is released, and the associated stress induced index changes are eliminated. Figure 10 shows the results of this procedure. Measurement and prediction of the effective indices of these annealed channel waveguides have the best agreement among the three fabrication cases. The processes have been repeated and the results are consistent, which indicates that this bleaching plus annealing technique allows for both predictability and process repeatability. For waveguides with the two smallest channel widths, the measured effective indices tends to be larger than those predicted. We have not found any other explanation except the speculation that with too narrow channel width, the assumption of rectangular waveguide geometry might not be valid any more. The surface profile across the channels of samples bleached at high temperature indicates that the stress on the boundaries are minimized, as shown in Figure 8b.

## IV. CONCLUSIONS

We have studied the effective indices of optical channel waveguides prepared by UV bleaching and compared them with the predictions from the effective indices of slab waveguides calculated by the effective index method. A special test structure for fabricating channel waveguides has been used for measurement and prediction consistency. UV bleached channel waveguides have been fabricated in three different ways: a) room temperature bleaching; b) high temperature bleaching; c) room temperature bleaching and high temperature baking (annealing). We find that measured effective indices of channel waveguides processed in way c) agree with the predictions from slab measurement better than those processed in a) and b). Causes of the major discrepancies in these two cases are stress induced index changes on the channel boundaries in a); and molecular diffusion

problems in b). The residual discrepancies between measurement and prediction may be caused by variations in the film thickness, uncertainties in the measured channel widths and the effective index measurement, and the assumption of a rectangular channel geometry. The accuracy of the effective index method has been verified for these channel waveguide dimensions through the computer simulation based on a semivectorial finite difference method[9], with the index distributions in the bleached film based on a UV bleaching model developed in our group. It seems important to continue to study the boundary effects of UV bleached channel waveguides if we hope to predict the channel waveguide performance from the knowledge of slab waveguides.

## V. ACKNOWLEDGMENTS

The authors would like to thank Jerry Swalen, Robert Miller and Don Burland from IBM Almaden Research Center for helpful advice and discussions. We would also like to give special thanks to Tony Logen from IBM Almaden Research Center for doing the AFM measurement of surface profile. The work is supported by a subcontract with IBM Almaden Research Center(ARC), subcontract number 70NANB2H1246, the IBM contract is funded by the Advanced Technology Program through National Institute of Standards and Technology. This work is also supported by IBM(ARC) through the Advanced Research Project Agency, subcontract number SUB-MDA972-93-1-0007, and by the Army Research Office under contract DAAL-03-92-G-0289.

FIGURE CAPTIONS

Figure 1 Schematic of the cross section of a UV bleached channel waveguide. The shaded area is covered by mask and is not bleached.

Figure 2 Effective index changes versus bleaching time for a high temperature bleached sample. The broadband UV light from a high pressure mercury lamp has an intensity of 68 $mW/cm^2$.

Figure 3 A flow chart of the effective index method.

Figure 4 A diagram of a bleached sample. The shaded areas are unbleached (the small ones represent the optical channels; the large one is considered to be unbleached slab region).

Figure 5 Three ways of realizing the M-line measurement of effective indices.

Figure 6 The detailed M-line measurement setup.

Figure 7 Effective indices of the fundamental modes of slab and channel waveguides UV bleached at room temperature. ——— represents the effective indices of the unbleached slab region, which is used to represent the slab indices of all the unbleached channel regions; —●— is the EIM calculations of the effective indices of these channels based on the slab measurements; ▫▫▫ represents the measured effective indices of the channel waveguides; ---o--- represents the effective indices of the bleached slab regions close to each of the channel waveguides. a) for TE polarization; b) for TM polarization.

Figure 8 The AFM surface profiles across a channel waveguide for samples, a) bleached at room temperature; b) bleached at a temperature close to the glass transition temperature of the polymer.

figure 9 The same as Figure 7, but with the sample bleached at 120 $^{o}$C.

Figure 10 The same as Figure 7, but with the sample bleached at room temperature and baked at 115 $^{o}$C for overnight.

TABLE 1 Agreement of the mesured effective indices of the channel wavguides with the calculations from slab waveguide measurements.

REFERENCES

[1] K.B. Rochford, R. Zanoni, Q. Gong, and G.I. Stegeman, "Fabrication of integrated optical structures in polydiacetylene films by irreversible photoinduced bleaching," Appl. Phys. Lett., 55, 1161(1989)

[2] M.B.H. Diemeer, F.M.M. Suyten, E.S. Trommel, A. McDonach, J.M. Copeland, L.M. Jenneskens, and W.H.G. Horsthuis, "Photoinduced channel waveguide formation in nonlinear optical polymers," Electron. Lett., 26, 379(1990)

[3] S. Immura, R. Yoshimura, and T. Izama, "Polymer channel waveguidex with low loss at 1.3 μm," Electron. Lett., 27,1342(1991)

[4] T. Kurihara, S. Tomaru, Y. Mori, and M. Hikita, "Third-order optical nonlinearities of a processable main chain polymer with symmetrically substituted tris-azo dyes," Appl. Phys. Lett., 61, 1901(1992)

[5] J. Trewhella, J. Gelorme, B. Fan, A.Speth, D. Flagello, and M. Oprysko, "Polymeric optical channel waveguides," Proc. SPIE 1377, 64(1990)

[6] R.M. Knox, and P.P. Toulios, "Integrated circuits for the millimeter through optical frequency range," Proceedings of MRI Symposium on Submillimeter Waves, J. Fox, Ed. (Polytechnic Press, Brooklyn, 1970)

[7] G.B. Hocker, and W.K. Burns, "Mode dispersion in diffused channel waveguides by the effective index method," Applied Optics, Vol.16, No.1, 113 (1977)

[8] Pao-lo Lin and Bing-Jin Li, "Semivectorial beam-propagation method for analysing polarized modes of rib waveguides," IEEE Journal of Quantum Electronics, Vol.28, No.4, 778(1992)

[9] M.S. Stern, "Semivectorial polarised finite difference method for optical waveguides with arbitrary index profiles," IEE Proceedings, Vol.135, Pt.J, No.1, 56(1988)

[10] N. Mabaya, P.E. Lagasse, and P. Vandenbulcke, "Finite element analysis of optical waveguides," IEEE Trans. Microwave Theory Tech., Vol.MTT-29, No.6, 600(1981)

[11] R.S. Moshrefzadeh, D.K. Misemer, M.D. Radcliffe, C.V. Francis, and S.K. Mohapatra, "Nonuniform photobleaching of dyed polymers for optical waveguides," Appl. Phys. Lett., 62(1), 16(1993)

[12] J.M. White, and P.F. Heidrich, "Optical waveguide refractive index profiles determined from measurement of mode indices: a simple analysis," Applied Optics, Vol.15, No.1, 151(1976)

[13] J. Helms, J. Schmidtchen, B. Schuppert, and K. Petermann, "Error analysis for refractive-index profile determination from nearfield measurements," J. Lightwave Technol., Vol. LT-8, No.5, 625(1990)

[14] J. D. Swalen, R. Santo, M. Tacke, and J. Fischer, "Properties of polymeric thin films by integrated optical techniques," IBM Journal of Research and Development, Vol.21, No.2, 168(1977)

[15] P.K. Tien, R. Ulrich, and R.J. Martin, "Modes of propagating light waves in thin deposited semiconductor films," Applied Physics Letters, Vol.14, No.9, 291(1969)

[16] Walter Charczenko, Ph.D. Thesis, University of Colorado, September, 1990

[17] R. Ulrich, and R. Torge, "Measurement of thin film parameters with a prism coupler," Applied Optics, Vol.12, No.12, 2901(1973)

[18] Submitted to J. Lightwave Technol.

[19] R. V. Ramaswamy, and R. Srivastava, "Ion-exchanged glass waveguides: a review", J. Lightwave Technol., Vol.6, No.6, 984(1988)

[20] J.W. Wu, "Birefringent and electro-optic effects in poled polymer films: steady-state and transient properties," J. Opt. Soc. Am., B/Vol. 8, No. 1, 142(1991)

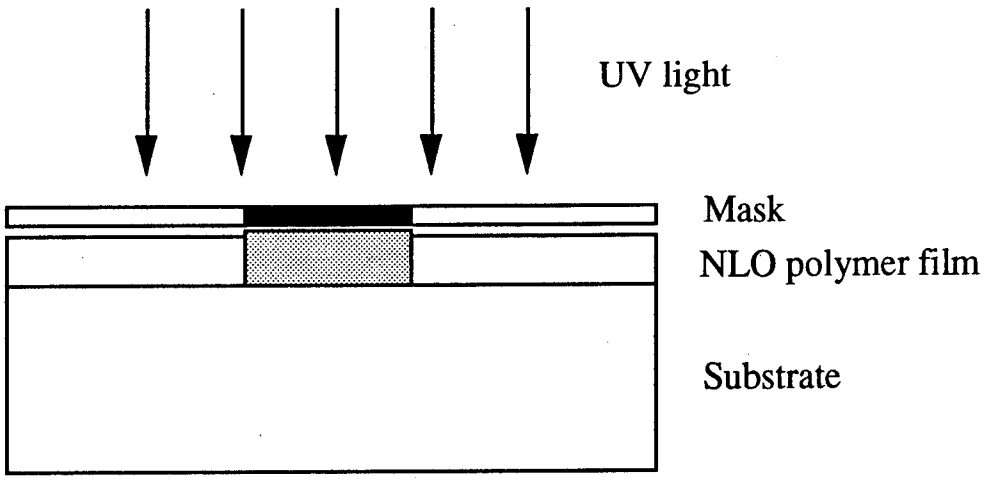


Figure 1

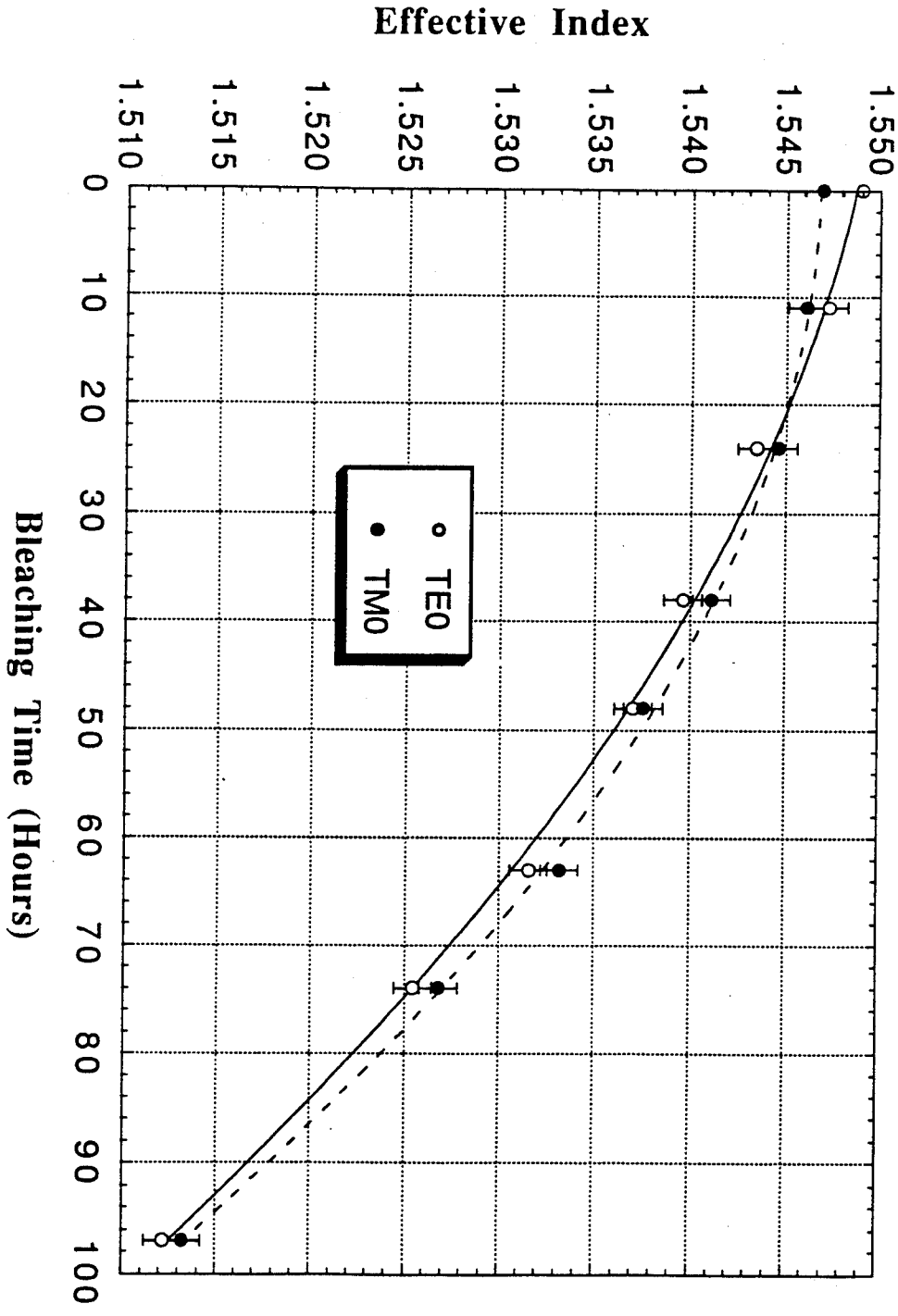
Effective Index
1.510
1.515
1.520
1.525
1.530
1.535
1.540
1.545
1.550
0
10
20
30
40
50
60
70
80
90
100
Bleaching Time (Hours)
TE0
TM0

Figure 2

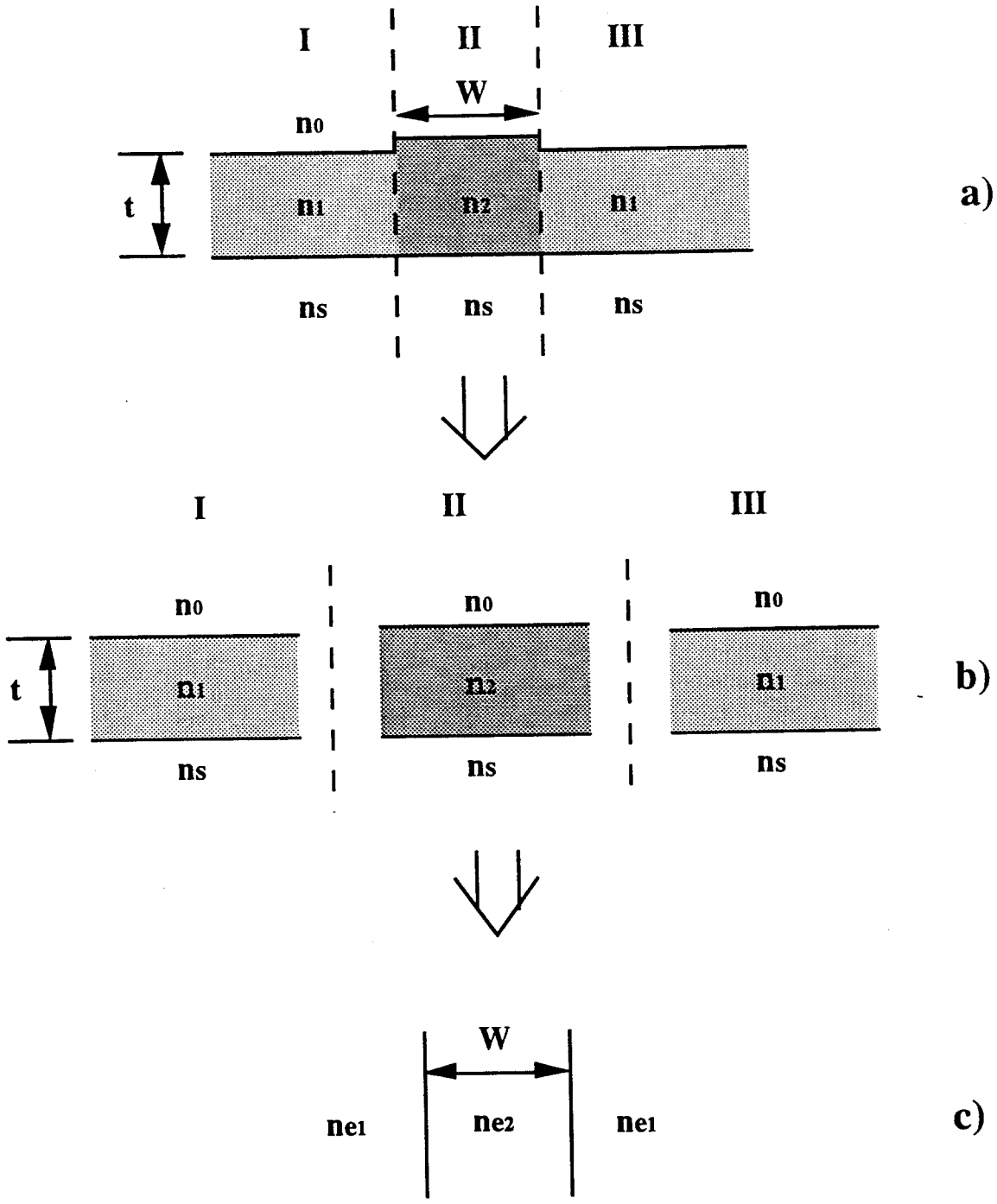
I
II
III
W
n0
t
n1
n2
n1
a)
ns
ns
ns
I
II
III
n0
n0
n0
t
n1
n2
n1
b)
ns
ns
ns
W
ne1
ne2
ne1
c)

Figure 3

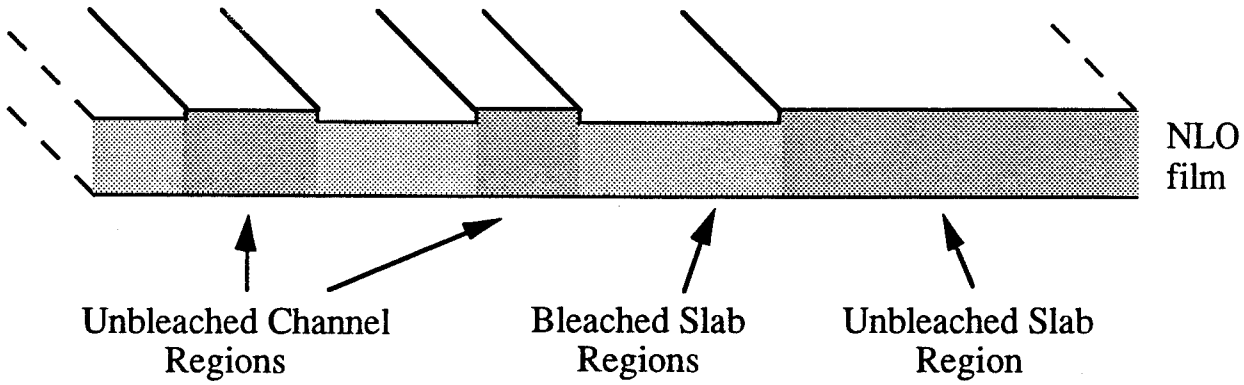
NLO
film
Unbleached Channel
Regions
Bleached Slab
Regions
Unbleached Slab
Region

Figure 4

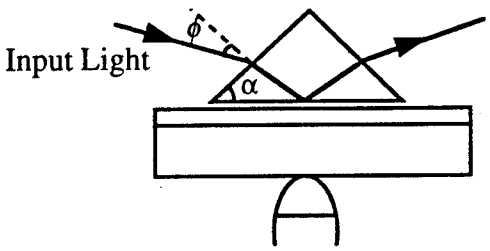


a)

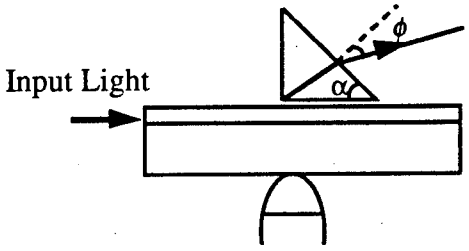


b)

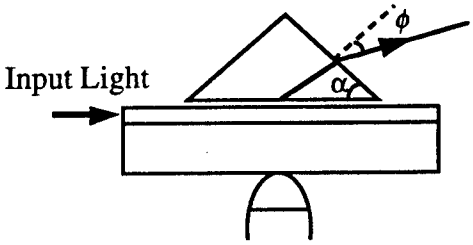


c)

Figure 5

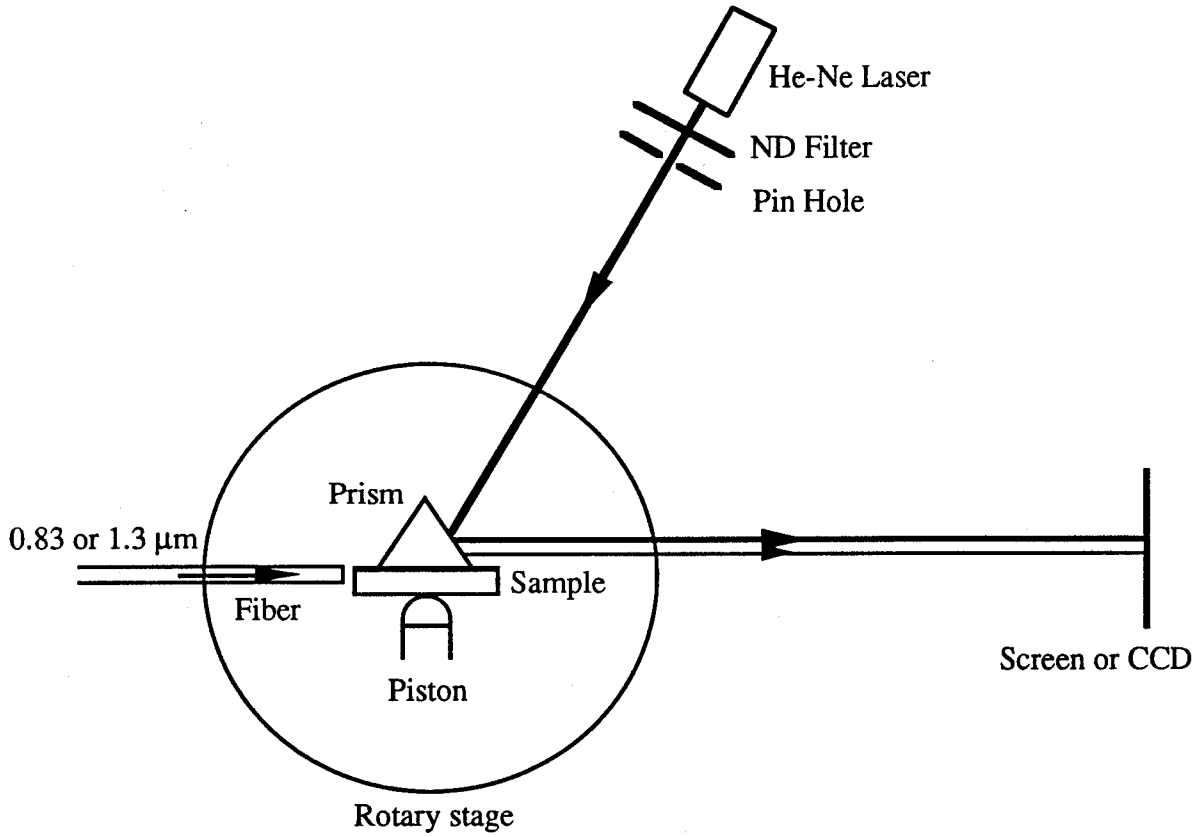
He-Ne Laser
ND Filter
Pin Hole
Prism
0.83 or 1.3 μm
Fiber
Sample
Piston
Screen or CCD
Rotary stage

Figure 6

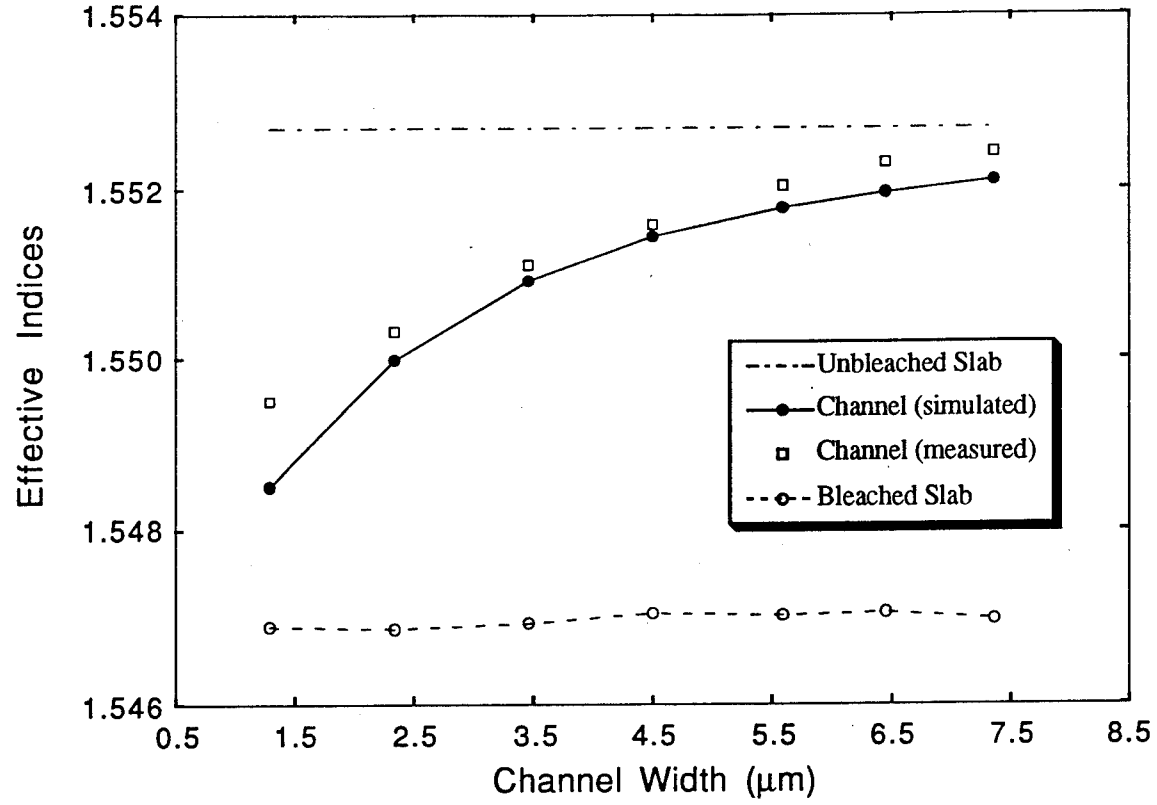
1.554
1.552
1.550
1.548
1.546
Effective Indices
0.5
1.5
2.5
3.5
4.5
5.5
6.5
7.5
8.5
Channel Width (μm)
Unbleached Slab
Channel (simulated)
Channel (measured)
Bleached Slab

a)

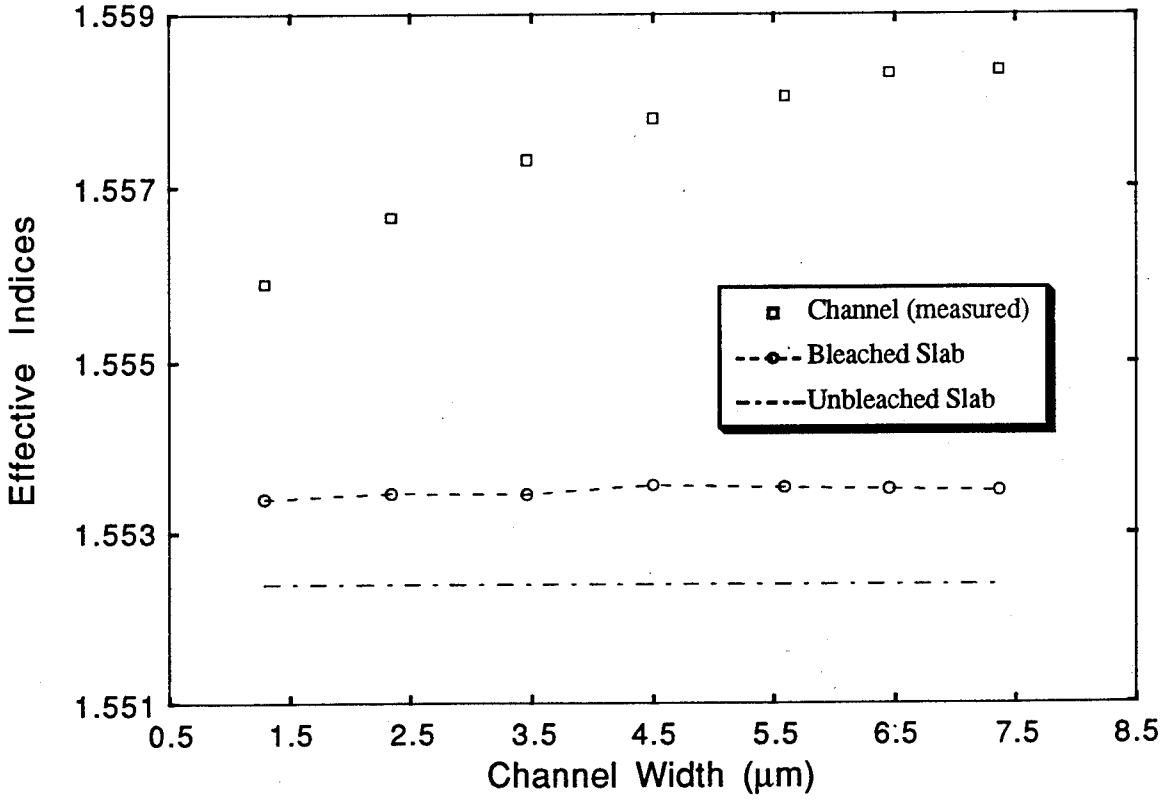
1.559
1.557
1.555
1.553
1.551
Effective Indices
0.5
1.5
2.5
3.5
4.5
5.5
6:5
7.5
8.5
Channel Width (μm)
Channel (measured)
Bleached Slab
Unbleached Slab

b)

Figure 7

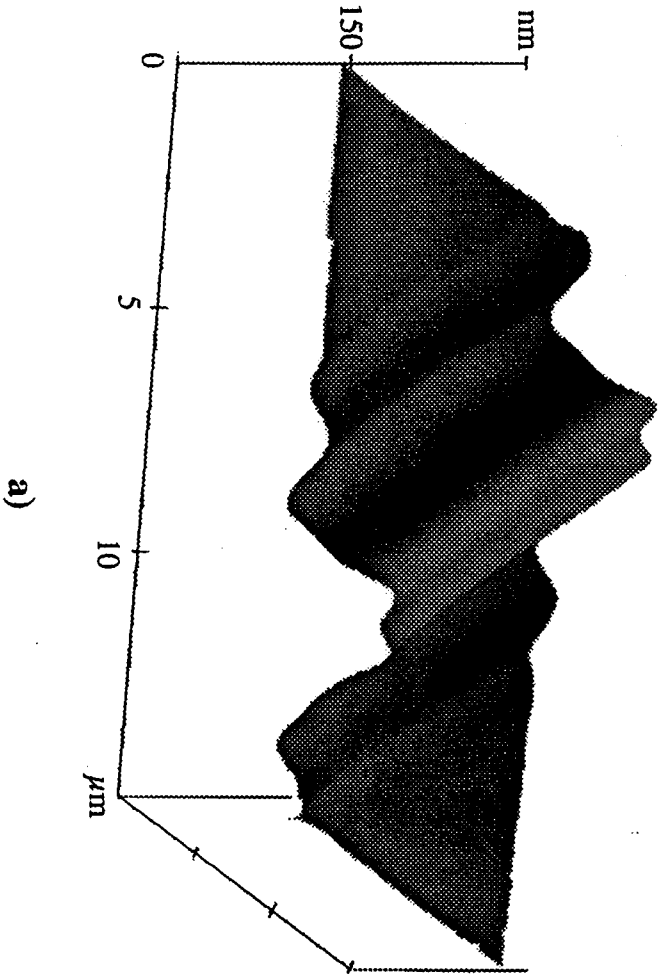


a)

Figure 8

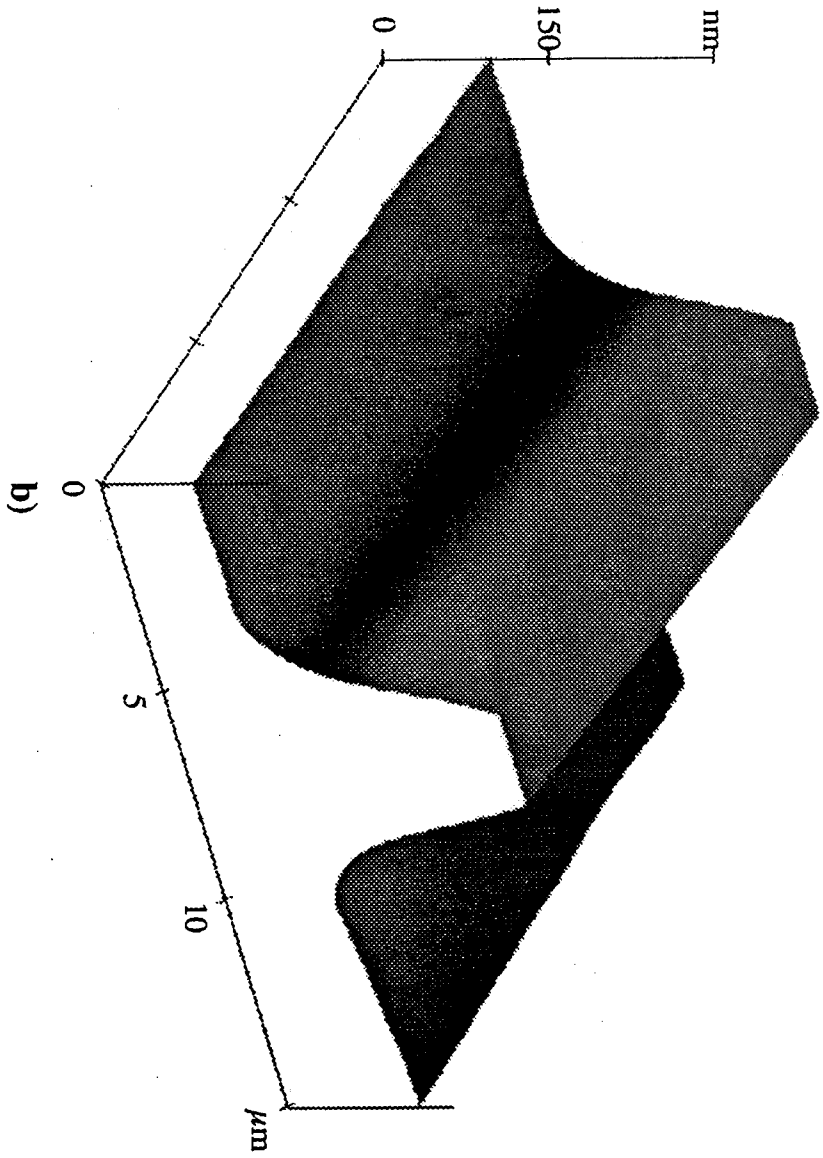


Figure 8

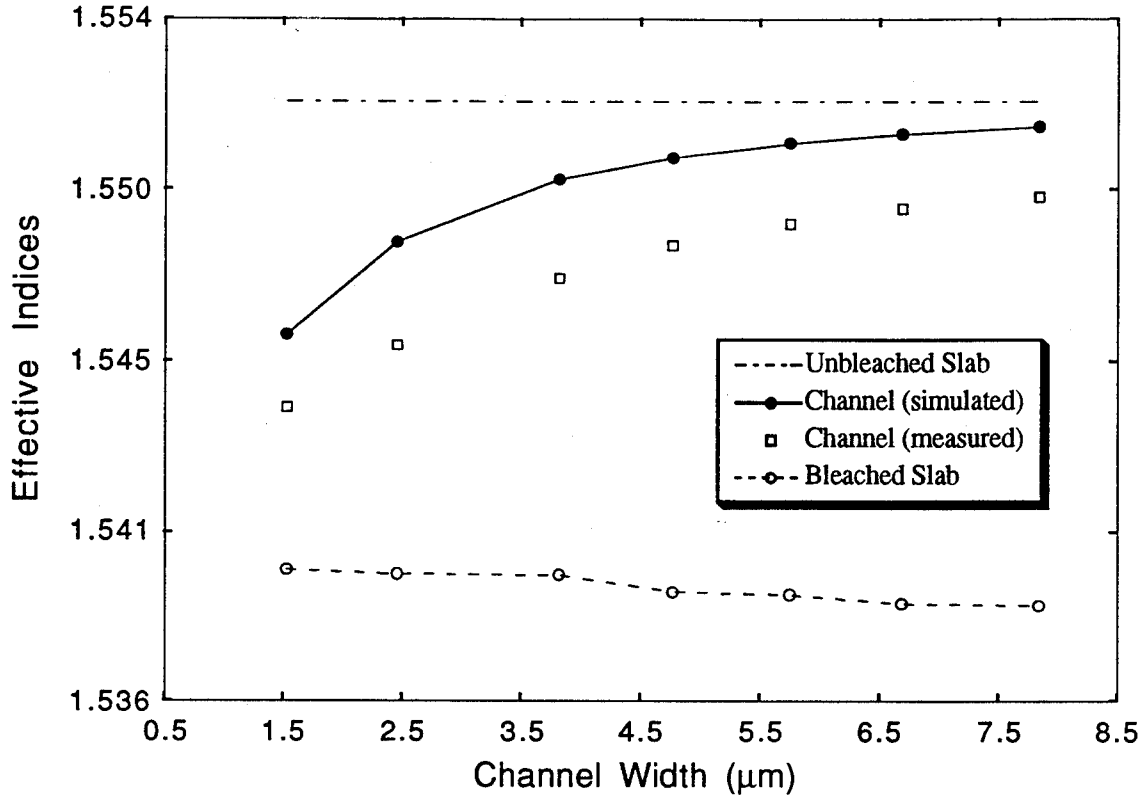
1.554
1.550
1.545
1.541
1.536
Effective Indices
0.5
1.5
2.5
3.5
4.5
5.5
6.5
7.5
8.5
Channel Width (μm)
Unbleached Slab
Channel (simulated)
Channel (measured)
Bleached Slab

a)

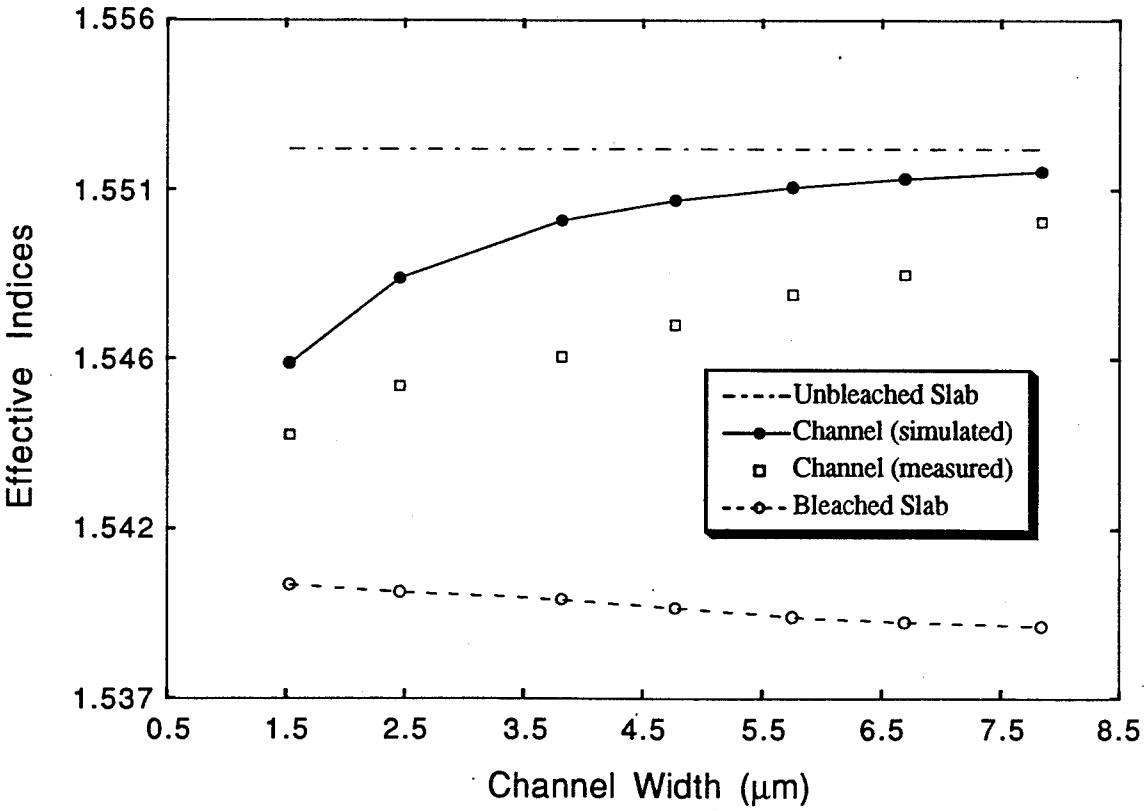
1.556
1.551
1.546
1.542
1.537
Effective Indices
0.5
1.5
2.5
3.5
4.5
5.5
6.5
7.5
8.5
Channel Width (μm)
Unbleached Slab
Channel (simulated)
Channel (measured)
Bleached Slab

b)

Figure 9

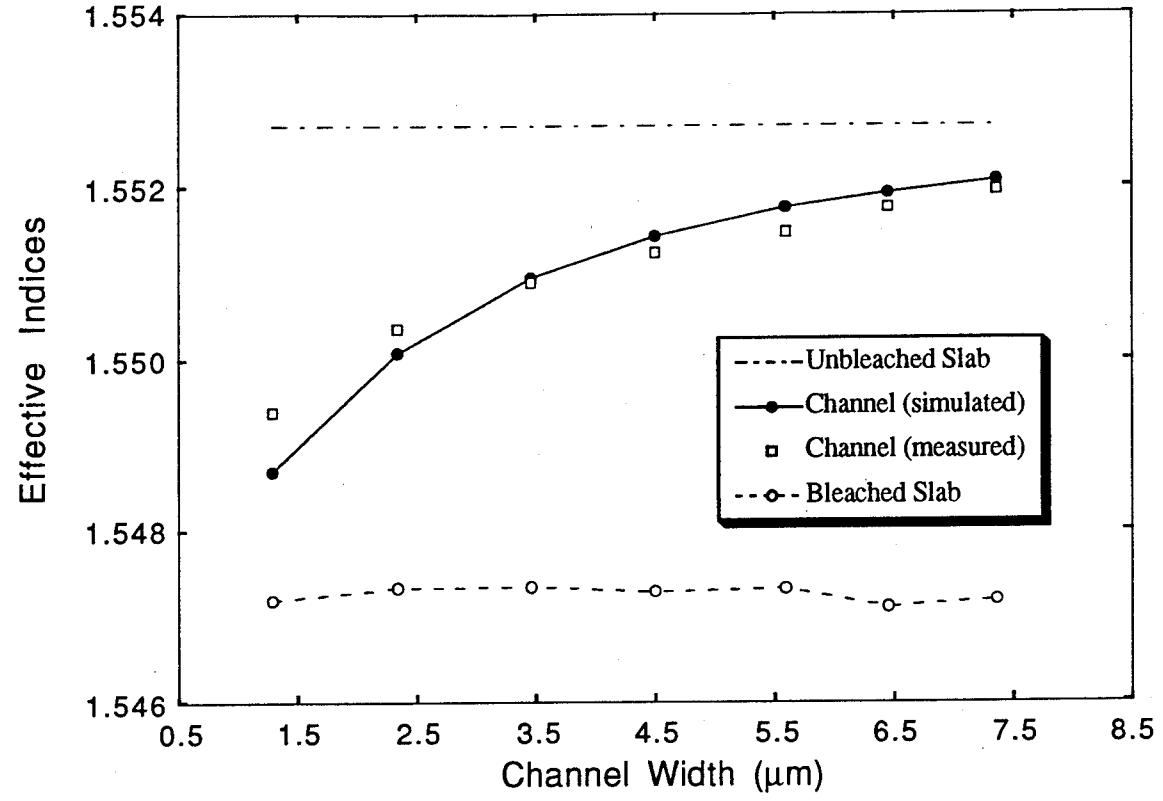
1.554
1.552
1.550
1.548
1.546
Effective Indices
0.5
1.5
2.5
3.5
4.5
5.5
6.5
7.5
8.5
Channel Width (μm)
Unbleached Slab
Channel (simulated)
Channel (measured)
Bleached Slab

a)

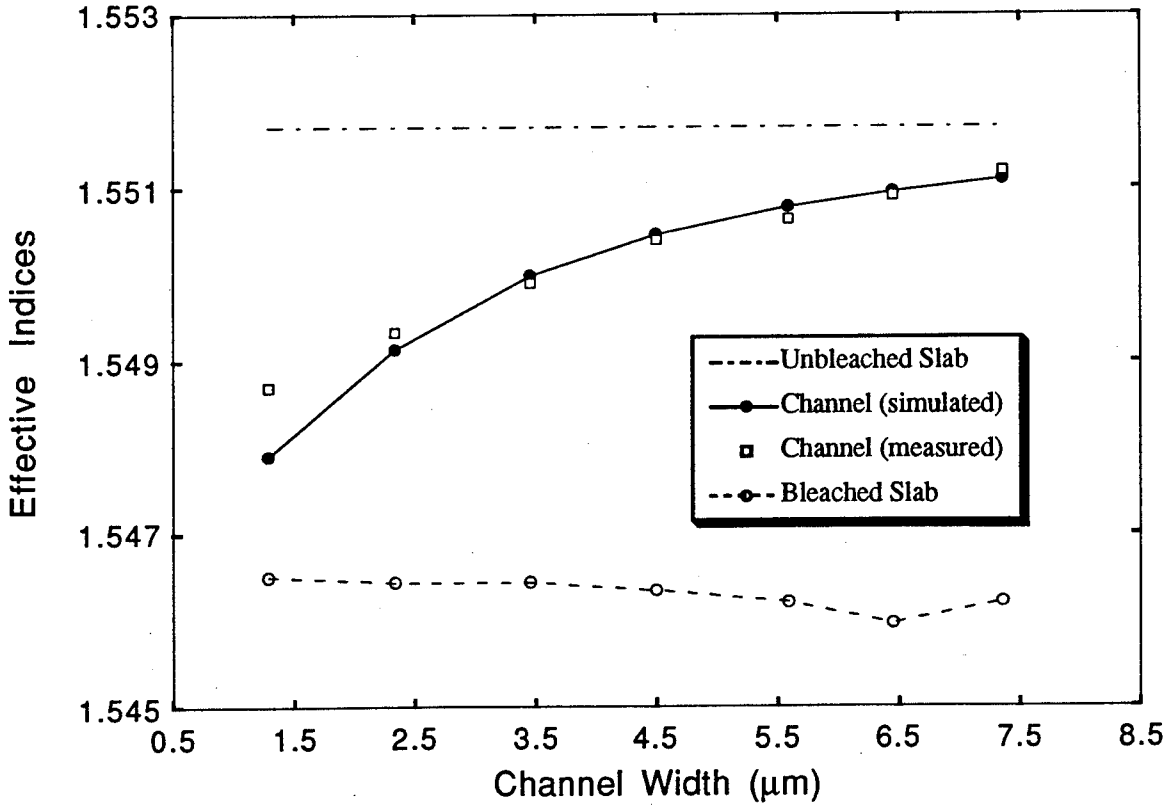
1.553
1.551
1.549
1.547
1.545
Effective Indices
0.5
1.5
2.5
3.5
4.5
5.5
6.5
7.5
8.5
Channel Width (μm)
Unbleached Slab
Channel (simulated)
Channel (measured)
Bleached Slab

b)

Figure 10

Table 1. Agreement of the measured effective indices of channel waveguides with the calculations from slab waveguide measurements.

| | Room Temperature | High Temperature | Room Temperature and Anealing |
|---|---|---|---|
| TE | Good | Poor | Good |
| TM | None | Poor | Good |